Design of a test rig for grease endurance tests

Results in Engineering 22 (2024) 102041

Contents lists available at ScienceDirect

Results in Engineering

journal homepage: www.sciencedirect.com/journal/results-in-engineering

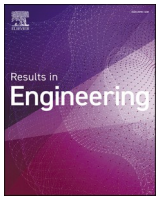

Design of a test rig for grease endurance tests

Edoardo Goti *, Francesca Maria Curà

Dipartimento di Ingegneria Meccanica e Aerospaziale, Politecnico di Torino, Corso Duca degli Abruzzi 24, 10129 Torino, Italy

A R T I C L E I N F O

Keywords:
grease
test rig
bearing
Endurance test
ECR

A B S T R A C T

Background: The performance and endurance of lubricating greases is often assessed through model tests (like four-ball tests or SRV tests). This approach has some limitations, especially when greases with special fillers are investigated, because simplified laboratory test conditions can never replicate real operating conditions.
Objective: For a more reliable assessment on the performance of a lubricating grease, lubricants must be tested in close-to-actual operational conditions, e.g. through component tests. This paper presents both the design and implementation of a dedicated test rig to test lubricating greases through middle-sized thrust ball bearings.
Methods: The test rig design is optimized to monitor the effectiveness of lubrication and determine the useful life of grease by recording representative parameters, namely bearing temperature at different location in the bearing, vibration level, and electric contact resistance (ECR) through the bearing.
Results: The results of a couple of assessment tests are presented and confirm that the test rig is working as expected.
Conclusions: The chart of the parameters being monitored shows that the instant performance of grease lubrication can be tracked during the endurance tests, and grease failure identified. The special mechanical layout of the rig also allows the user to obtain additional information that is usually not available in other commercial greased bearing testers. This work is meant to be the first step of the development a new approach to evaluate the grease lubrication performance and a few experimental results are included as they are intended as a functional validation of the prototyped test rig.

1. Introduction

Several testing methods belonging to the group of the simplified 'model test' (as per the definition provided by the DIN 50322 standard) are widely used for testing greases, e.g., four-ball test (Shell VKA test machine), pin-on-disc test, Almen-Wieland test, SRV high-frequency reciprocating test, two-disc (or twin disc) test, to mention but a few [1]. These methods are currently used in the development process of lubricants to allow for rapid and economical determination of changes in the main lubricant characteristics through the development stages.

However, it is hard to predict the actual performance of lubricants based on the results of simplified tests only because the correlation between these and the actual applications is not straightforward [2]. This especially holds in the case of special greases, e.g. greases functionalized by innovative fillers of solid-nano particles. No type of *simplified model test* can reproduce the same working conditions of real applications, although representative values of speed, contact pressure and operating temperature (or environmental temperature) can be reproduced in laboratory tests for higher significance [3]. In other words, the more the tribological test is simplified, the lower it can be susceptible to the whole set of influencing factors and phenomena involved in the real applications.

For a more reliable assessment on the performance of grease, lubricants must be tested in close-to-actual operational conditions of real applications, e.g. by *component tests* exploiting a suitable component. Optimizing the lubricant performance for real applications is possible, indeed, only if the lubricants can be tested under conditions matching practical use. Rolling element bearings are a class of mechanical components particularly suited for testing the grease performance. It is known from the extensive literature on the topic that rolling element bearings are susceptible to the lubrication regime [4] and the quality of the lubricant additive package. Grease "ages" in grease-lubricated bearings, and the service life of the component is very often determined by the life of the grease itself, making the grease and bearing duration closely interlinked.

Many standardized lubricant testing methods are based on rolling

* Corresponding author.
E-mail address: edoardo.goti@polito.it (E. Goti).

https://doi.org/10.1016/j.rineng.2024.102041
Received 15 November 2023; Received in revised form 22 January 2024; Accepted 13 March 2024
Available online 16 March 2024

bearing test rigs, e.g. FE8 and FE9, which follow the DIN 51819 and DIN 51821 standard respectively, the R0F + testing method by SKF, the LFT testing method by FAG [5]. Also, the SNR-FEB2 (Fafnir) fretting testing method according to ASTM D4170 for the evaluation of false brinelling phenomena is exploited to assess the protection of grease against wear in bearings [6]. Many other customized test rigs have been developed by researchers in the scientific field for specific purposes, for instance Refs. [7–9].

This paper presents both the design and implementation of a dedicated test rig to test lubricating greases through middle-sized thrust ball bearings and to assess the duration and effectiveness of lubrication.

The test rig allows to monitor all those testing parameters useful to determine the state of health and the effectiveness of lubrication of grease, namely bearing temperature, ECR thought the bearing, and vibration level. Contrary to other commercial bearing testers, where the performance of greases is usually inferred based on the life of the bearing itself, this test rig allows to detect the failure of the lubrication mechanism before the eventual structural failure of the bearing. This is a plus especially when special greases (greases functionalized by innovative fillers of solid-nano particles) are investigated, for instance graphene-enriched greases. The use of this customized test rig fulfils the need to perform endurance tests in the framework of an ongoing research activity on graphene-enriched greases carried on by the authors [10–13].

This paper is the output of more than 1 year of development before the prototyped test rig could be operated. Section 2 and 3 are devoted to the description of the test rig, its conceptualization, and its design characteristics. The mechanical layout was conceived so that any adaptation of this test rig to other types of rolling bearings is possible, in case of need. Section 4 presents the results of some preliminary tests with two thrust bearings of different size to validate the proper functioning of the prototyped test rig.

This work is the 1st step of the development a new approach to evaluate the grease lubrication performance, and this explains why just a few results are presented through this work.

2. Conceptualization of the test rig

Thrust ball bearings were chosen among other rolling element bearings because they have fully decoupled rings and rolling elements. This makes it easy to inspect the contact surfaces under an optical microscope and with a profilometer while looking for contact fatigue and damage accumulation inside the raceways, and greasing of the component is straightforward as well. Moreover, a single load is to be applied to fully stress the component to its typical operating conditions, which also simplifies the layout of the test rig compared to a mixed radial and axial loading scenario.

The main requirements for the test rig were defined in the conceptualization stage and are listed as follows.

- ❖ The test rig should allow the use of a small-sized thrust ball bearing. Testing of grease with overly large bearings is avoided to minimize costs, reduce complexity in design and simplify the in-house assembly on the test rig itself.
- ❖ The applied load must be high enough to accelerate the accumulation of damage and reduce the duration of the tests, i.e. testing should occur above the endurance fatigue load limit P_U of the bearing.
- ❖ The driving motor and the support bearings should be able of medium-to-high speed regimes, i.e. at least 3000 rpm, representative of typical industrial applications such as small grease-lubricated gearboxes. However, the overly high rotational speed is usually not of interest for ordinary grease-lubricated bearings under high loads due to excessive viscous heating and thermal instability above the thermal reference speed of bearings.
- ❖ The temperature of the bearing used for testing should be measured during the tests, as well as ECR to monitor the lubrication regime.
- ❖ Vibration and noise levels from running the endurance tests should be minimized.
- ❖ The bearing greased with the grease under test should be visible to observe the grease redistribution and to make non-contact temperature measurements by IR camera possible on the static ring, rotating ring, on the cage, and on the grease build-up around the cage.
- ❖ One bearing greased with the grease under test should be tested at a time.
- ❖ The test rig should feature a flexible mechanical layout for simple adaptation to other kinds of bearing testing, also with other types of rolling bearings, in case of need.
- ❖ The support bearings and the other auxiliary bearings of the test rig should be large enough to carry the test loads without any significant damage during the whole testing campaign, even considering off-design scenarios.
- ❖ Test rig, acquisition software, the control system and safety shutdown system should allow long-term unsupervised 24/7 accelerated tests.

3. Design of the test rig

3.1. Mechanical layout

The mechanical layout of the test rig specifically designed for this research activity was inspired by the standard industrial rolling bearing grease testers and some dedicated bearing test rigs for research purposes found in the scientific literature. Among others, it is worth citing similar test rigs implemented by Alegranzi et al. [14], Niknam et al. [15], He et al. [16], Cao et al. [17], Fan et al. [18] and the one recently appeared in the paper by Nassef et al. [19]. Fig. 1a shows the section view of the test rig, while Fig. 1b presents the CAD model in full axonometric view. The main shaft (① in Fig. 1) is supported by two bearing units Dodge P2B-GTMAH-50 M. The main technical specifications of the support bearings are listed in Table 1. Pillow block bearing units were selected to reduce the manufacturing cost of the test rig dramatically. The selected bearing units are manufactured according to the requirements of air-handling applications, i.e. they feature reduced vibration and noise level, improved shaft guidance for high-speed running and can operate cooler for longer grease life.

In the actual prototype of the test rig, contact seals of the bearing units limit the maximum speed during the endurance tests to 4300 rpm. However, the very same bearing units may also be manufactured with labyrinth seals which guarantee smooth running up to higher speed. The maximum rotational speed of the tests could be easily extended to 6700 rpm in the future, if needed, by replacing the bearing units with those featuring labyrinth seals. This performance was deemed satisfactory since the adjusted reference speed of the target thrust bearings used to run the grease endurance tests is usually lower than this limit [20], especially when the test load exceeds the endurance fatigue load limit P_U. Previous evidence suggested that acceleration of bearing endurance tests should occur through a load increase rather than an increase of speed, for thermal reason [21].

The location of the shaft into the bearing was assured by a pull/push adapter system (Dodge grip-tight®) that enables fully concentric positioning of the shaft. It is optimized for high rotational speed and high loads to reduce vibrations due to misalignments.

At the left end of the hollow shaft, the thrust ball bearing exploited to test grease ② (Fig. 1a) is installed coaxially to the shaft. The test rig was designed to allow testing on thrust bearings with a minimum bore equal to 20 mm.

The bell-shaped component ③ in contact with the fixed ring of the tested bearing applies the axial load of the test and is connected to a 10 kN load cell (HBM U2B) ④. The cylinder ⑩, which can slide axially, is used to align the axis of the component ③ with the axis of the main shaft

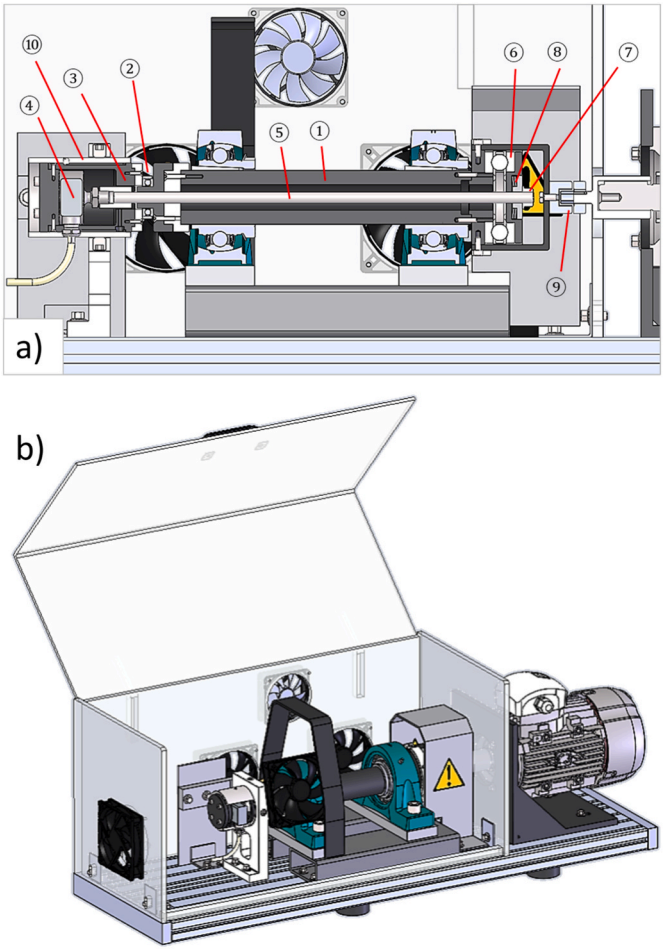

Fig. 1. (a) Section view of the test rig; (b) CAD model of the test rig for grease testing.

① before running the test.

The threaded tie rod ⑤ coaxial with the main shaft connects the load cell with the static ring of a 51309 thrust ball bearing ⑥ installed on the right end of the shaft (whose specs are reported in Table 1). This auxiliary thrust bearing decouples the rotating parts of the test bench from the static loading system and allows for balancing the axial load without loading the two support bearings.

Fan et al. [18] first proposed to apply an internally balanced axial load that exploited a dedicated 4-rod loading frame surrounding the rotating part of their test rig. The solution adopted in the present test rig aims at simplifying this concept. The loading frame is replaced by the threaded tie rod coaxial to the main shaft, which guarantees compact dimensions and a significant reduction in the complexity of the layout. The presence of such coaxial loading element limits however the minimum size of the bearings that can be used for the tests, whose inner bore should be at least 20 mm.

The load is not applied through an external actuator, but the user sets by tightening a lock nut ⑦ that forces the rolling elements and the thrust rings into close contact. Two Belleville springs ⑧ (size 40x20.4 × 2mm, nominal load 5730 N) are placed in a series arrangement behind the lock nut to add compliance to the loading line. The Belleville springs allow accurate setting of the initial thrust load and compensate for thermal expansion due to frictional heating during operation.

Table 1
Support and auxiliary bearings data from manufacturer.

Data		DODGE P2B-GTMAH-50 M	SKF 51309
Bore	[mm]	50	45
Basic dynamic load rating	[kN]	43.4	76.1
Basic static load rating	[kN]	29.3	153
Limiting speed	[rpm]	4300	4000
Reference speed	[rpm]	–	2800
Fatigue limit	[kN]	–	5.6

Fig. 2 compares the original solution by Fan et al. with the schematic representation of the simplified solution designed for this test rig. This simplified solution has some cons, in any case. Tight machining tolerances are required to guarantee the concentricity of components along the loading line; otherwise, undesired vibration would occur. Moreover, the test rig is ready for testing bearings under axial loads only which is indicated if thrust ball bearings or angular contact ball bearings are exploited, not for deep groove ball bearings. Also tapered roller bearings are not indicated because a much higher load would be needed to exceed the fatigue limit of this class of bearings.

The connection with the 3 kW three-phase asynchronous electric drive Lafert AMPE 90L DA2 is provided by a flexible jaw coupling ⑨. The electric drive is operated with a 4 kW inverter ES350-F0-2K2G/4K0P–3B from Cumark Co.Ltd that allows the continuous regulation of the motor speed from 25Hz up to 100Hz in open loop mode. Since the torque output of the drive is the result of the bearing friction only, the inherent rotor slip is supposed to be limited during operation. The actual rotational speed of the shaft (ω_{test}) during tests was then calculated according to equation (1), where 3000 rpm is the rotational speed of the magnetic field at a nominal excitation frequency of 50 Hz and 2865 rpm the related idling speed of the rotor. The calculation is based on the simplifying assumption that the ratio between the nominal speed of the magnetic field and the rotor speed is constant at any excitation frequency $f_{inverter}$, because the rated load to the motor is very low and limited to the rolling torque of bearings:

$$\omega_{test} = f_{inverter} \bullet 60 \bullet \frac{2865}{3000} \; [rpm] \tag{1}$$

A polycarbonate safety enclosure (visible in Fig. 1b) protects the rotating parts of the test bench and houses cooling fans. Preliminary testing showed that the tested bearing quickly ran into overheating at 1500 rpm inside the enclosure because the test speed was higher than the thermal reference speed of the bearing, and the applied load exceeded the rated fatigue limit. Therefore, an active air-cooling system was designed with four 200 CFM cooling fans to control the temperature of the tested bearing. One cooling fan forces fresh air to enter the testing chamber from one side, two fans installed at the level of the pillow blocks take the hot air out of the test chamber, and one fan installed inside forces recirculation of fresh air around the bearing under test (Fig. 3).

The support bearings of the bearing units work under no radial load except for the own weight of the components. They are insensitive to the axial load F_A by design. This feature makes the duration of these bearings theoretically unlimited. However, the concept behind the mechanical layout of the test rig was also to allow testing on radial bearings in the future with minimum layout adaptations. In the presence of external loading on a radial bearing under test, a couple of fixture reaction forces would rise on the support bearings. Therefore, the position of the support bearings was optimized to extend the bearing life, considering the presence of a virtual radial load F applied at one extremity of the shaft. In particular, the relative distance between the two support bearings SB1 and SB2 and the applied radial force, i.e. the l, l_1 and l_2 in Fig. 4, was calculated to minimize the load carried by the most loaded bearing (bearing SB2). F_B is reduced by increasing l and reducing l_2. Considering the need for compactness and other functional requirements, l was fixed to 198 mm and l_2 to 67 mm.

The testing parameters and the related bearing rating life for the P2B-GTMAH-50 M support bearings are presented in Table 2, where a_{SKF} is the life modification factor [20] and η_C is the grease contamination factor according to the ISO 281:2008 standard. The *Design scenario* refers to a testing condition where the speed is 1500 rpm, i.e. the nominal

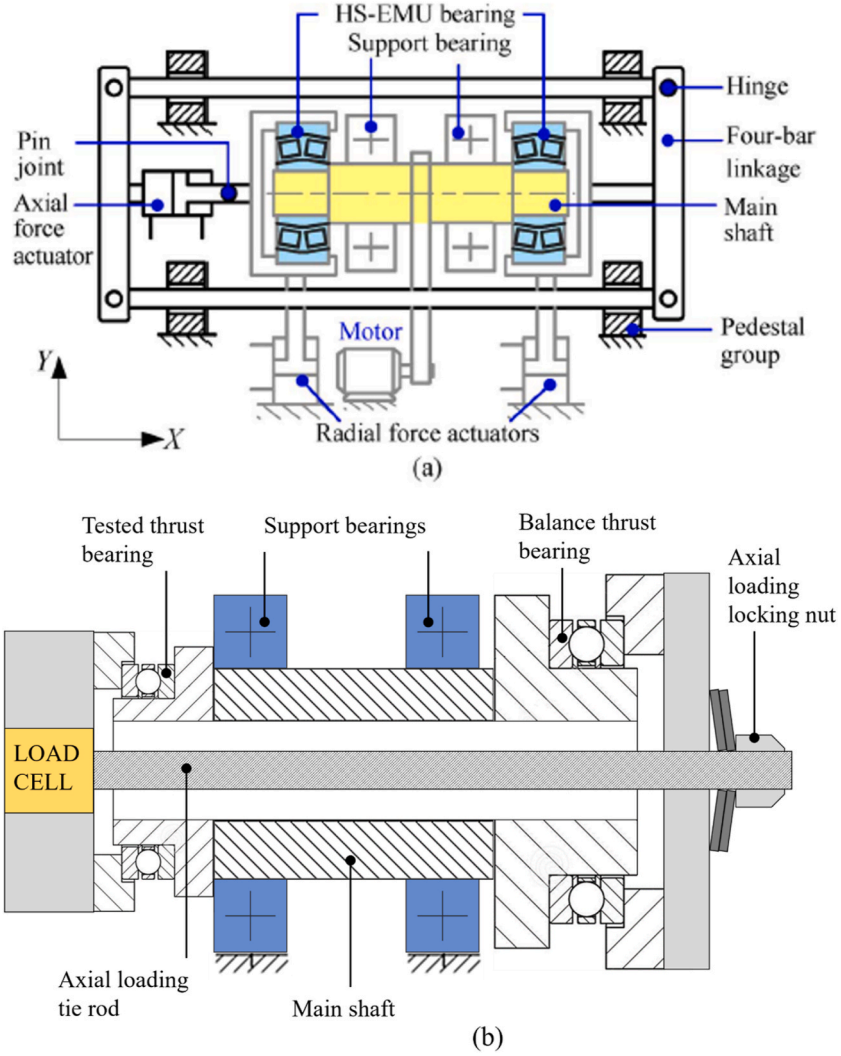

Fig. 2. (a) Schematic of the test bearing for HS-EMU bearings by Fan et al. [18]; (b) schematic of the loading system implemented in this test rig.

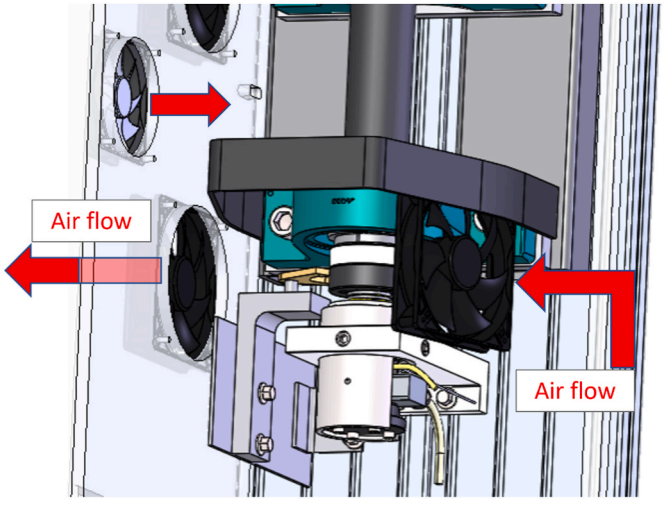

Fig. 3. Air-cooling system of the bearing to avoid overheating due to accelerated-life endurance test conditions.

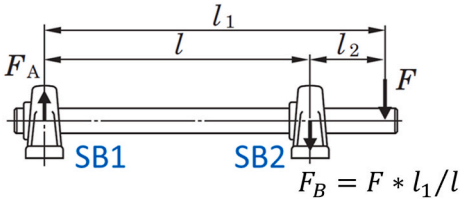

Fig. 4. Schematic of the reaction forces on the support bearings SB1 and SB2 for the scenario where an external radial load acts on the bearing under test (adapted from KYH Mounted Bearing Units Catalogue, Nippon Pillow Block Co. Ltd., https://www.fyhbearings.com).

working speed of this test rig, and the bearing used to test grease would be a deep groove ball bearing with a 5 kN load applied radially. A 0.5 kN thrust load was included to account for parasitic axial load due to the thermal expansion of the shaft (the support bearings are both locating by design). The off-design scenarios refer to a possible working condition of the support bearings with higher speed and higher load.

The estimated life of the support bearings in this testing condition is still virtually unlimited. The off-design scenarios consider two hypothetical testing conditions where the support bearings operate under higher load and speed. The minimum estimated bearing life exceeds 500 days, which is satisfactory for a test bench.

Table 2
Equivalent bearing life calculations of P2B-GTMAH-50 M. Calculations were carried out through the SKF Bearing Select online calculation tool for bearings.

	Design scenario	Off-design scenario	Off-design & high speed	
Axial force	0.5	0.5	0.5	kN
Radial force F	5	9	9	kN
F_B	5.4	12.0	12.0	kN
C/P	8.72	4.84	4.84	–
Speed	1500	1500	3000	rpm
Inner ring T	60	60	60	°C
Outer ring T	60	60	60	°C
Grease	NLGI2 Li–C	NLGI2 Li–C	NLGI2 Li–C	–
η_C	0.85	0.85	0.85	–
Shaft	Horizontal	Horizontal	Horizontal	–
a_{SKF}	37.9	9.6	9.6	–
$\mathbf{L_{10m}}$	$>2*10^5$	12100	6060	h
Estimated life	8000	504.2	252.5	days
Relubrication	13400	6470	3370	h
Power loss	99	138	290	W

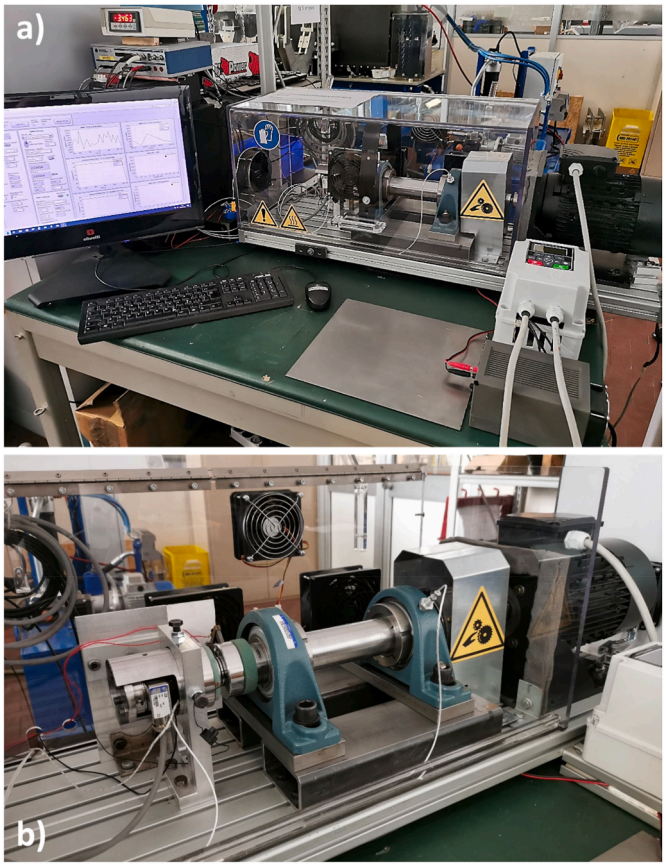

Fig. 5. Pictures of the prototype of the test rig at the Laboratory of Mechanics (DIMEAS, Politecnico di Torino).

Fig. 5 shows the prototype at the Laboratory of Mechanics of DIMEAS Politecnico di Torino.

3.2. Data acquisition, control, and emergency shut-down system

The control and data acquisition system of the test rig were self-developed using LabView®. A LabView routine with a dedicated GUI was implemented for this test rig. The logical framework of the control and the data acquisition system is schematized in Fig. 6. The testing parameters being monitored while running the grease endurance tests are as follows.

- ❖ Temperature of the static ring of the bearing used for grease testing measured in a single location.
- ❖ Temperature of the static ring of the support bearing measured in a single location.
- ❖ Electric Contact Resistance (ECR) through the bearing under test.
- ❖ Applied axial load.
- ❖ Axial vibrations.

Fig. 7 is the detailed view of the sensorized bearing seat. The temperature of the bearing used for grease endurance tests was sensed by a Resistance Temperature Detector (RTD) of the Pt100 type. A dedicated pre-loaded micro temperature sensor was designed according to the schematic shown in the inset of Fig. 8. Tests did not run under controlled temperature conditions but under self-induced frictional heating, contrary to standardized bearing endurance tests. The tiny size of the sensor guarantees good responsiveness to limited temperature variations and a relatively fast response time. Fig. 8 shows how the temperature sensor was installed at the level of the bearing seats into a blind hole and in direct contact with the static ring of the test bearing. Measurement of temperature at a single location of the static ring was deemed satisfactory due to the relatively small size of the bearing; the distribution of temperature into the ring is expected nearly uniform in steady-state conditions.

The temperature of the support bearings was measured with a commercial temperature sensor for pillow blocks installed into the grease nipple hole and in contact with the outer ring of the bearing. 3-wire RTD sensors were chosen due to the high stability of the measured values and the high immunity to electromagnetic interference. Each sensor was conditioned by a 24V DC-powered temperature transducer, which converts the electrical resistance fluctuations in a 4–20 mA current signal from 0 °C to 300 °C. The current level associated with the temperature values was acquired with the amperemeter integrated into the National Instruments VirtualBench VB-8012 device with a sampling rate equal to 5Hz.

The resolution of the electrical current reading was ±30 μA, which allows measuring the temperature level with a resolution of about ±0.5 °C. A digital safety stop condition based on temperature was coded inside the LabView-based control software to avoid undesired overheating of the bearing under test. The safety stop criterion activates a DO channel of the VirtualBench wired to a DI channel of the inverter, and it stops the test in case of overheating.

A uniaxial accelerometer was installed close to the temperature sensor to detect the axial vibration behind the bearing seat (Fig. 7). Data from the accelerometer were acquired at 4 kHz through a Bruel & Kjier Nexus 2693 amplifier and analysed in real time during the test. The PSD of the acceleration signal in the time domain was calculated in the frequency range from 0 Hz to 2 kHz. The average of 10 subsequent PSD charts was stored in memory every 10 min to track the evolution of the power spectrum during the test.

The ECR system was intended to monitor the electric resistance through the lubricated rolling contacts between the balls and the raceway.

The 2-wire measurement of the electric resistance is performed through the Digital MultiMeter (DMM) integrated into the same NI VirtualBench VB-8012 device, whose measuring specifications are reported in Table 3. With the 2-wire method one can obtain the broadest measuring range out of the DMM, i.e. from 0.001Ω to 100 MΩ, with auto-ranging enabled by the control software of the instrument. The ECR value measured through this setup also includes the bulk resistance of the rings, the resistance of the electrical line, of soldered connections and connectors and that of the sliding brush. However, any other terms except the resistance thorough the lubricated point contacts are deemed to have negligible fluctuations during the tests.

Two insulating plates made of Vetronite FR4 (Uciesse Spa, Leinì, Italy) are placed behind the static and rotating ring of the bearing, as shown in Fig. 9a. These plastic plates made of high-strength and high-

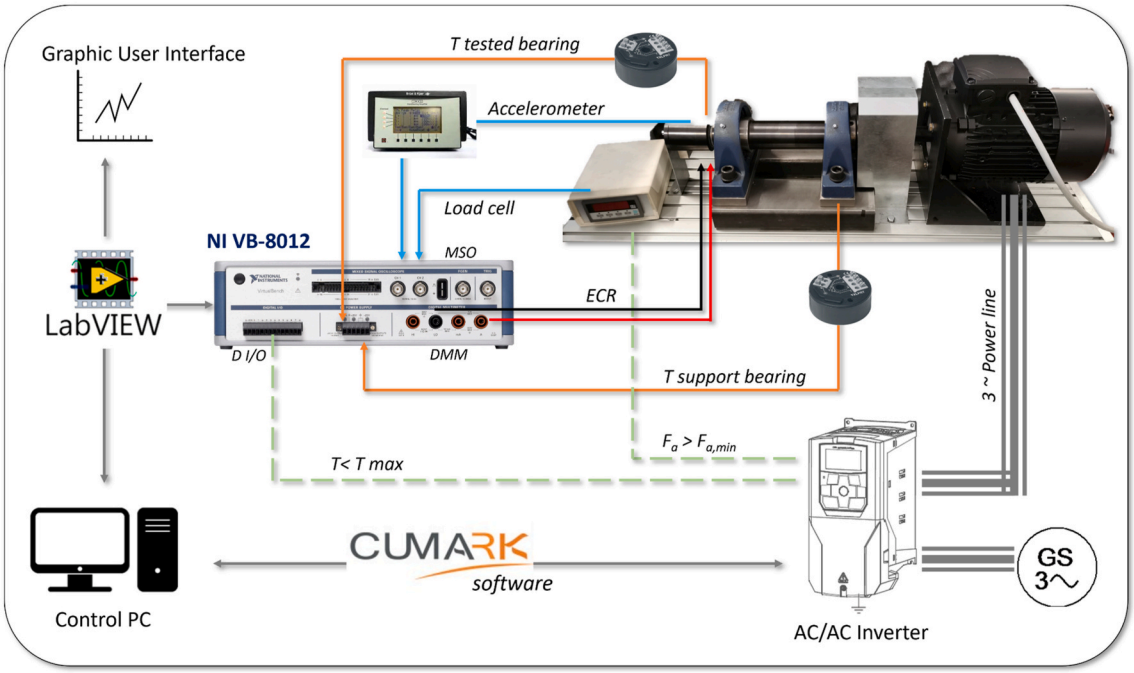

Fig. 6. Schematic of the control and data acquisition system of the test rig.

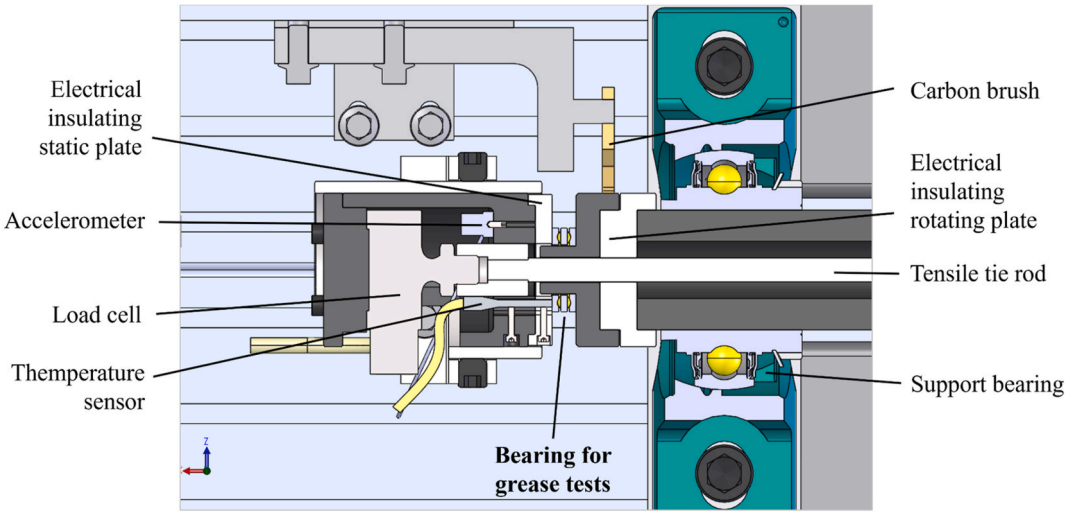

Fig. 7. Section view of the sensorized seat of bearing under test. Sensor type and mounting is represented in a simplified way in the CAD model; details are provided in Fig. 8.

thermal-stability engineering polymer insulate the region where the ECR measurement is performed from the rest of the test bench to avoid any electrical current dispersion through the test rig frame.

The static ring was connected to the DMM through a wire directly soldered to the ring, visible in Fig. 10. Soldering was necessary to avoid disturbances and interference in the electrical measurement due to vibrations and grease nearby.

A couple of carbon brushes for electrical application slide against a mirror-finished steel surface next to the seat of the bearing under test. The carbon brush allows to close the electrical circuit at the rotating side of the bearing. The characteristic resistance of the sliding contact was verified in the setup phase of the test rig by connecting the pole of the DMM ohmmeter normally connected to the static rig of the bearing to a second carbon brush sliding against the same rotating surface. The characteristic electrical resistance thus measured was stable and in the order of few Ohms, which is negligible compared to the values usually measured during an endurance test (see for instance Fig. 12).

The rotating ring of the bearing is glued to its seat with a special electrically conductive glue rich in Ag powder to improve conduction at the bearing-seat interface.

The HBM U2B load cell is connected to a Druck DPI 280 transducer which linearizes the 0–10 kN measuring load range into a 0–5 V voltage signal. The oscilloscope acquires the voltage signal (MSO) integrated into the VirtualBench device and sampled at 1 Hz. An additional safety emergency stop criterion was implemented by wiring a DO port of the Druck process transduced to one of the DI channels of the inverter. If the axial load lowers below a given threshold set by the user, the drive stop running to protect the test bench in the event of failure of the axial tie rod or load loss due to other misfunctioning.

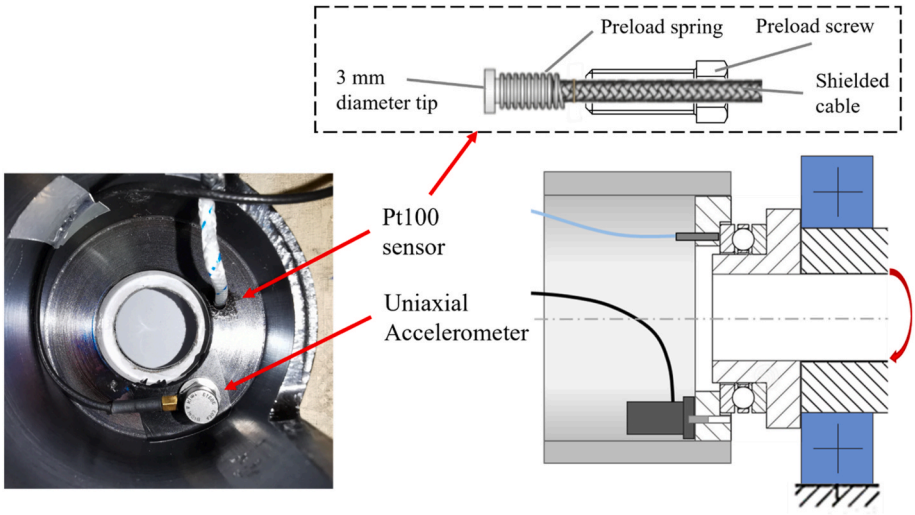

Fig. 8. Sensorized seat of the bearing under tests featuring the customized temperature sensor and the uniaxial accelerometer. The schematic of the customized micro-temperature sensor specifically designed for this test rig is presented in the upper part of the figure.

Table 3
Measuring range and accuracy of the Digital MultiMeter in DC Resistance mode (2-Wure, 1V Open Circuit Voltage) installed into the National Instrument VirtualBench VB-8012 multifunction card [22].

Range	Short-Circuit Current	1-Year Accuracy ± (% of Reading + % of Range)	Temperature Coefficient ± (% of Reading + % of Range)/°C
100 Ω	170 μA	0.018 + 0.050	0.0010 + 0.0005
1 kΩ	170 μA	0.018 + 0.005	0.0010 + 0.0005
10 kΩ	70 μA	0.018 + 0.005	0.0010 + 0.0005
100 kΩ	10 μA	0.018 + 0.005	0.0010 + 0.0005
1 MΩ	1.1 μA	0.035 + 0.005	0.0040 + 0.0005
10 MΩ	1.1 μA	0.150 + 0.005	0.0100 + 0.0005
100 MΩ	1.1 μA	1.300 + 0.005	0.1000 + 0.0005

4. RESULTS of preliminary tests

Two preliminary endurance tests were carried out to assess the regular operation of the test rig. A commercial SKF 51105 thrust ball bearing (25 mm bore, 42 mm outer diameter, 16 spheres 6 mm in diameter) and a SKF 51104 thrust ball bearing (20 mm bore, 35 mm outer diameter, 14 spheres 5.55 mm in diameter). Bearing with a bore larger than 20 mm can be installed into the test rig through a centering bushing.

Both bearings were tested as purchased. Bearings were greased with MULTEMP ET-C high-performance bearing grease by Kyodo Yushi Co. Ltd. The testing parameters and the results of these preliminary endurance tests are summarized in Table 4. The axial load corresponded to a contact pressure below 3.5 GPa, which is the limit of permanent plastic deformation [21]. The average conformity of the raceways was measured by measuring the raceway profile with a stylus profilometer in four different positions of the rolling path of the spheres. Both tests run with steady-state speed of 1500 rpm after a run-in period lasted 1h where the speed was gradually increased from 500 rpm to 1500 rpm to avoid peaks of temperature. Air cooling was activated to limit overheating of the thrust bearing used for the test, since the test speed exceed the calculated adjusted reference speed in both cases.

The quantity of lubricating grease applied was *2 g*, according to the quantity suggested by the SKF Bearing Select online calculation tool [23]. The corresponding volume was determined with a precision scale featuring 0.1 mg resolution (KERN ALJ220-4NM). Greasing procedure was carried out by evenly spreading grease on the rings and on the cage separately, before the load is applied. No relubrication occurred during the tests.

Both tests were periodically stopped and resumed to monitor the evolution of the interface state and the grease degradation by means of a

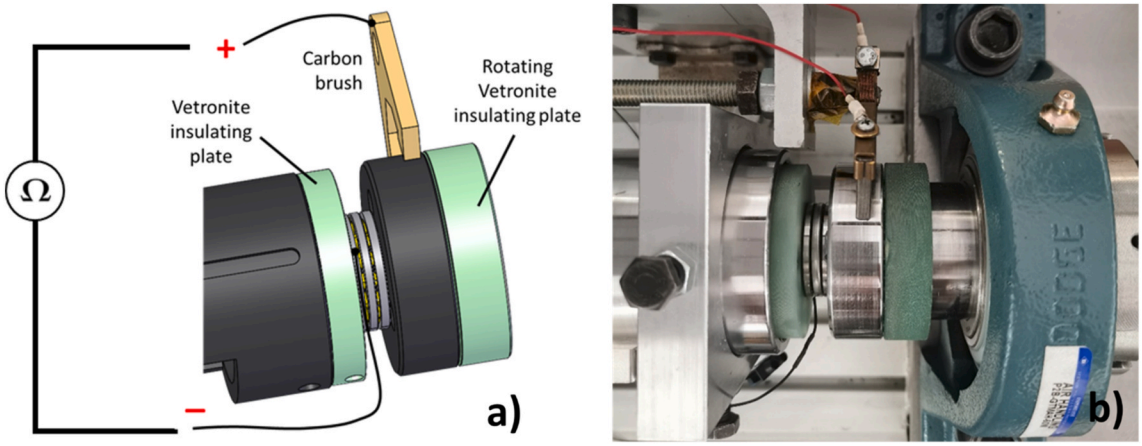

Fig. 9. (a) Insulting plates for ECR measurement made of Vetronite FR4; (b) Detailed of the bearing installed on the test rig to run a test and connected to the ECR system.

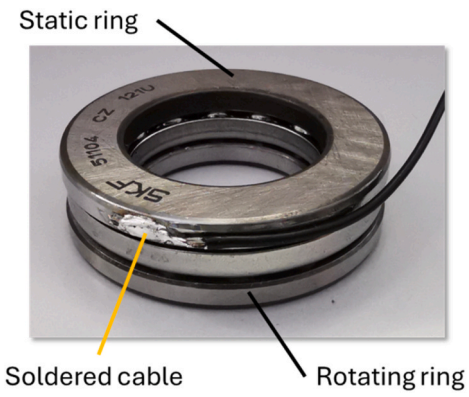

Fig. 10. ECR wire tin-soldered to the static ring of a 51104 bearing.

Table 4
Preliminary tests data. Grease failure was arbitrarily set when the temperature of the bearing static ring exceeded 95 °C.

Data		Test 1	Test 2
Bearing code	–	51105	51104
Average axial load	[kN]	9.41	8.13
Speed	[rpm]	1500	1500
Adjusted reference speed [20]	[rpm]	1270	1330
C/P (SKF Catalogue)	–	1.96	1.84
Average conformity of the raceways	–	0.537	0.546
Estimated L_{10mh} (SKF Bearing Select)	[h]	73	55
Duration	[h]	330	199
Average temperature of the static ring	[°C]	70.4	71.5
Average ECR	[MΩ]	2.73	3.84
Stop condition	–	Test aborted	Grease failure

visual inspection. Figs. 11 and 12 show the curves of temperature and ECR recorded during the two tests.

The diagrams show that a slight variation of the monitored parameters was observed during the whole test after the running-in period. The working temperature of the bearing stabilized between 70 and 72 °C with air cooling activated and featured occasional spikes to 75–80 °C after 100 h. Transitory loss of grease performance was associated with these fluctuations, because the ECR (Fig. 13) signal dropped to low values every time a peak of temperature was observed. No damages were detected on the raceways and on the balls by the end of the two tests, and no signs of structural failure.

Test 1 was stopped once the cumulative duration exceeded a threshold duration reasonable for laboratory tests, which was far higher than the theoretical L_{10} life ratings calculated according to ISO 281:2008 (see Table 4). before a lubricant failure condition was observed. In the case of Test 2, the arbitrary condition of grease failure (T > 95 °C & ECR <0.1% of the average ECR value) was reached after about 200 h.

These results suggest that thrust ball bearings of size 51104 are more expedient for future repetitions of these endurance tests with the selected grease, because the test duration is significantly reduced.

Fig. 13a shows the time series of the average PSD signal stored in memory every 10 min from the beginning to the end of Test 1. The PSD chart did not show any significant alterations of the frequency response within the frequency range being considered, which is meaningful considering that no evidence of failure of the grease lubrication mechanism was observed in Test 1. In the case of Test 2, on the other hand, an increased vibration level at the end of the test indicated that the contact condition was unstable during the last part of the test. Fig. 13b compares the average PSD chart of axial vibrations after 1h of test with that at the end corresponding to the stop the test. A distributed increase of the PSD intensity in the whole frequency range followed a generalized increase in the noise level and agreed with the alterations of the values of temperature and ECR indicated in Fig. 11.

5. Conclusions

This paper presented the design of a test rig optimized for grease endurance tests. The mechanical layout of the test rig aimed at simplifying the system and reducing costs, while allowing a comprehensive monitoring of the rolling bearing used to carry out the grease tests. The test rig was designed to test greases through thrust ball bearings with minimum inner fore of 20 mm, maximum axial loading of 10 kN, and maximum rotational speed of 4300 rpm. However, its mechanical layout was conceived to extend its application range to higher load and speed and to other types of rolling bearings with limited adaptations of the layout, for instance, by adding a radial force actuator to allow for testing deep grove ball bearings.

The results of the preliminary tests presented in Section 4 suggest that the test rig is working as expected and that it is suitable for research on lubricating greases. Useful information about the lubrication mechanism can be obtained from the monitored signals, which make it possible to detect grease failure, according to relevant criteria for the specific application of interest. In the case of the validation tests presented above, a threshold condition was set on the temperature of the static ring of the bearing used for the tests and on the electrical resistance drop through the same bearing.

The special mechanical layout also allows one to obtain additional information that is rarely available in other commercial greased bearing testers, e.g. the distribution of the grease mass can be studied since the

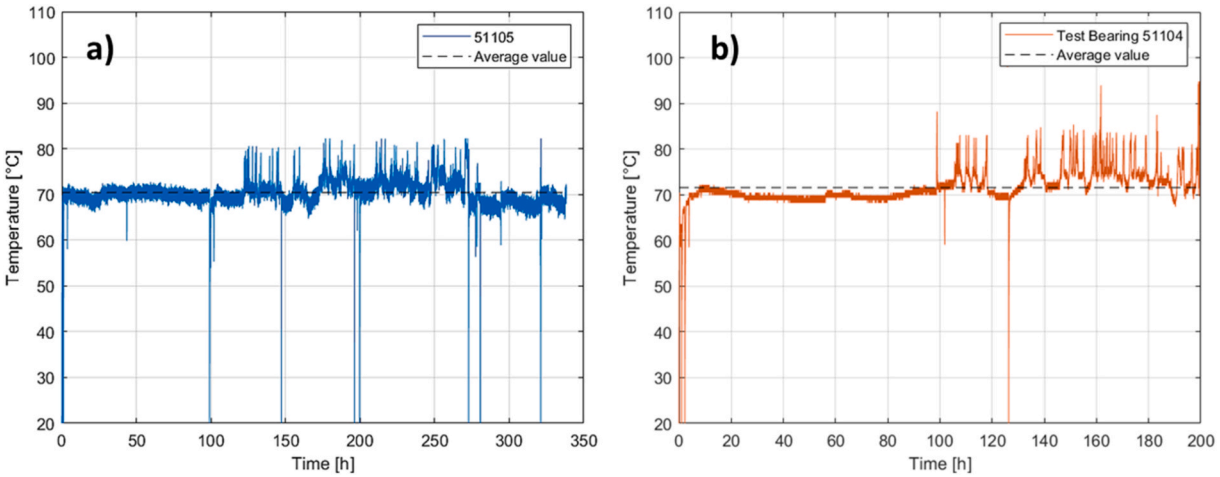

Fig. 11. Temperature chart recorded during (a) Test 1 with a 51105 bearing; (b) Test 2 with a 51104 bearing.

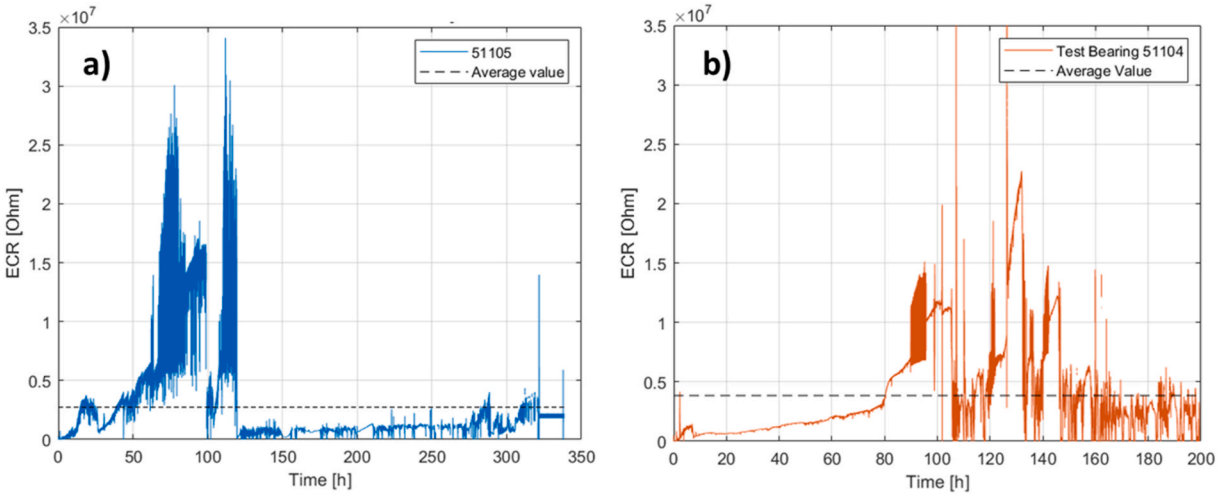

Fig. 12. ECR chart recorded during (a) Test 1 with a 51105 bearing; (b) Test 2 with a 51104 bearing.

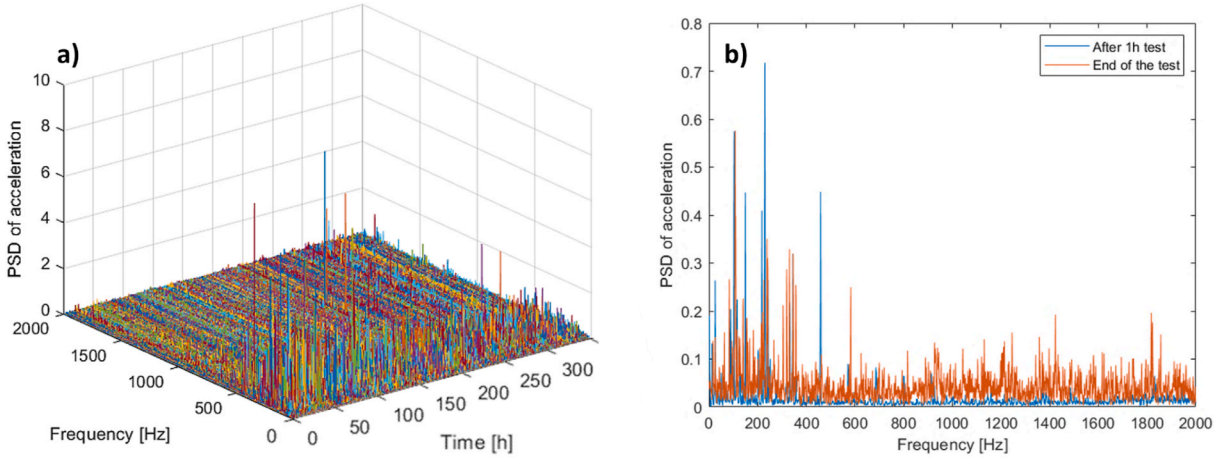

Fig. 13. (a) Series of the average PSD signal in the frequency domain recorded during Test 1; (b) Comparison between the PSD after 1h of test and at the end of Test 2.

test bearing is exposed. Moreover, the grease temperature could be directly measured at different bearing locations in non-contact mode through an IR camera to broaden the performance analysis to the thermal behaviour of the contact interface.

What is presented in this paper is just the 1st step of a broader investigation in which such a new approach to test the grease performance will be applied. This justifies the reason why just a few results are presented in Section 4 since they are just meant as a functional validation of the prototyped test rig. In the framework of the ongoing research activity, the authors are planning an extended experimental campaign with this rig to test the performance of graphene-enriched greases, i.e. greases where nanoflakes of graphene are added as a functionalizing additive. In fact, graphene-enriched greases have been extensively tested through simplified model tests in recent years (like SRV tests [24–26], or four-ball tests [27–29]) but, to the best of the authors knowledge, their performance has never been verified through component tests in the scientific literature.

Statement and DECLARATION

The authors declare that the submitted work is original, it is not under consideration for publication elsewhere, and that all the authors gave explicit consent to submit this work to the journal.

All authors certify that they have no affiliations with or involvement in any organization or entity with any financial interest or non-financial interest in the subject matter or materials discussed in this manuscript.

Moreover, the authors declare that they did not receive support from any organization for the submitted work.

CRediT authorship contribution statement

Edoardo Goti: Conceptualization, Data curation, Investigation, Methodology, Validation, Writing – original draft. **Francesca Maria Curà:** Formal analysis, Project administration, Resources, Supervision, Writing – review & editing.

Declaration of competing interest

The authors declare that they have no known competing financial interests or personal relationships that could have appeared to influence the work reported in this paper.

Data availability

Data will be made available on request.

References

[1] G. Straffelini, Friction and Wear, Springer, 2015.
[2] Lubrication of Rolling Bearings. pag 156-166, Schaeffler Technologies AG & Co KG, 2013.
[3] J.P. Blau, Friction Science and Technology: from Concepts to Applications, CRC Press, 2009.
[4] P. Lugt, A. Van den Kommer, H. Lindgren, C. Roth, The R0F+ Methodology for Grease Life Testing, SKF Industries, 2013.
[5] S.E. Klüber Lubrication, K.G. Co, Lubricant Testing - Focusing on Mechanic-Dynamical Tests, München, 2017.
[6] C. Lu-Minh, P. Njiwa, K. Leclerc, et al., Effectiveness of greases to prevent fretting wear of thrust ball bearings according to ASTM D4170 standard, Results in Engineering 14 (2022) 100468.
[7] T. Cousseau, B. Graça, A. Campos, J. Seabra, Experimental measuring procedure for the friction torque in rolling bearings, Lubric. Sci. 22 (2010) 133–147.
[8] J. Takabi, M.M. Khonsari, Experimental testing and thermal analysis of ball bearings, Tribol. Int. 60 (2013) 93–103.
[9] M. Scherge, R. Böttcher, D. Kürten, D. Linsler, Multi-phase friction and wear reduction by Copper Nanopartices, Lubricants 4 (No. 36) (2016).
[10] A. Mura, F.M. Curà, F. Adamo, Evaluation of graphene grease compound as lubricant for spline couplings, Tribol. Int. 117 (2018) 162–167.
[11] E. Goti, F. Curà, Friction torque in thrust ball bearings lubricated by graphene-enriched grease with a modified pin-on-disc method, International Journal of Mechanics and Control 24 (1) (2023) 207–214.
[12] A. Mura, F.M. Curà, F. Adamo, Tribological performance of graphene-nanoplatelets as grease additive, 6° Workshop AIT "Tribologia e Industria", 18-19, April 2018. Torino, Italy.
[13] E. Goti, L. Corsaro, F.M. Curà, Tribo-thermo-electrical Investigation on Lubricating Grease Enriched with Graphene Nano-Platelets as an Additive, Wear, 2024. *Accepted paper*.
[14] S. Alegranzi, J. Gonçalves, H. Gomes, Ball bearing vibration monitoring for fault detection by the envelope technique, Blucher Mechanical Engineering Proceedings 1 (n. 1) (2014).
[15] S. Niknam, V. Songmene, J. Joe Au, Proposing a new acoustic emission parameter for bearing condition monitoring in rotating machines, Trans. Can. Soc. Mech. Eng. 37 (4) (2013) 1105–1114.
[16] D. He, R. Li, M. Zade, J. Zhu, Development and Evaluation of AE Based Condition Indicators for Full Ceramic Bearing Fault Diagnosis, 2011 IEEE Conference on Prognostics and Health Management, 2011, pp. 1–7.
[17] L. Cao, F. Sadeghi, L.-E. Stacke, A Wireless sensor Telemeter for in-Situ cage vibration measurement and Corroboration with Analytical results, Tribol. Trans. 61 (6) (2018) 1013–1026.
[18] B.-Q. Fan, K.-M. Lee, X. Ouyang, H.-Y. Yang, Soft-switchable Dual-PI controlled axial loading system for high-speed EMU Axle-Box bearing test rig, IEEE Trans. Ind. Electron. 62 (12) (2015).
[19] M. Nassef, M. Soliman, B. Nassef, et al., Impact of graphene nano-Additives to Lithium grease on the Dynamic and tribological behavior of rolling bearings, Lubricants 10 (29) (2022).
[20] SKF Rolling Bearings Catalogue, SKF Group, 2021.
[21] T. Harris, Rolling Bearing Analysis, John Wiley & Sons, 2001.
[22] NI VirtualBench VB-8012 User Manual, National Instrument, 2014.
[23] SKF Bearing Select , www.skfbearingselect.com/, SKF Industries.
[24] J. Wang, X. Guo, Y. He, M. Jiang, et al., Tribological characteristics of graphene as grease additive under different contact forms, Tribol. Int. 127 (2018) 457–469.
[25] X. Fan, Y. Xia, L. Wang, et al., Multilayer graphene as a lubricating additive in Bentone grease, Tribol. Lett. 44 (3) (2014) 455–464.
[26] M. Xie, J. Cheng, C. Huo, G. Zhao, Improving the lubricity of a bio-lubricating grease with the multilayer graphene additive, Tribol. Int. 150 (2020) 106386.
[27] T. Ouyang, Y. Shen, R. Yang, L. Liang, et al., 3D hierarchical porous graphene nanosheets as an efficient grease additive to reduce wear and friction under heavy-load conditions, Tribol. Int. 144 (2020) 106118.
[28] B. Kamel, A. Mohamed, M. El Sherbiny, K. Abed, et al., Tribological properties of graphene nanosheets as an additive in calcium grease, J. Dispersion Sci. Technol. 38 (10) (2017) 1495–1500.
[29] B. Lin, I. Rustamov, L. Zhang, J. Luo, X. Wan, Graphene-reinforced Lithium grease for Antifriction and Antiwear, ACS Appl. Nano Mater. 3 (2020) 10508–10521.